Heterogeneous Catalysis

DOI: 10.1002/anie.201206720

Sulfur and Nitrogen Dual-Doped Mesoporous Graphene Electrocatalyst for Oxygen Reduction with Synergistically Enhanced Performance**

*Ji Liang, Yan Jiao, Mietek Jaroniec, and Shi Zhang Qiao**

The oxygen reduction reaction (ORR) is a key process in energy conversion and storage in, for example, fuel cells[1] and metal–air batteries[2] as well as in other applications including water purification, oxygen detection, and corrosion protection.[3] In lithium–air batteries and low-temperature fuel cells ORR takes place almost exclusively on Pt/C catalysts at the cathode. However, the high price, sluggish ORR process, intolerance to fuel crossover, and instability of the Pt/C catalyst in the fuel-cell environment have greatly impeded the commercialization of fuel cells and limited their performance.[1] Therefore, extensive studies have been conducted to find alternative metal-based catalysts with or without Pt, which could be viable from an economical viewpoint; however, current results are far from satisfactory.[4,5] Thus, there has been great interest in the development of metal-free catalysts for ORR. For this purpose, N-doped carbons have been extensively studied. Their potential for ORR originates from the heteroatoms present in the graphitic framework, which make these catalysts non-electron-neutral and consequently favors the molecular adsorption of oxygen and its reduction. Although moderate ORR performance has been obtained on these materials, their ORR activity is still inferior to that of conventional Pt/C catalysts.[6,7]

Among carbon materials, graphene, the ultrathin two-dimensional network composed of sp^2-hybridized carbon atoms, has become a very popular candidate for ORR catalysis because of its high conductivity and excellent mechanical properties,[8] which are greatly favorable for the harsh ORR process. Recently, other elements besides N (e.g. B, S, and I) have been introduced into graphene.[9–11] Although these newly developed doped-graphene materials have shown better performance than the N-doped materials, the improvement in the ORR catalytic activity has been very limited owing to the low content of the doped elements. To address this issue, some researchers have proposed to dope graphene with both B and N to further improve the ORR catalytic activity, since this is controlled not only by the increased number of dopant heteroatoms but also by the synergistic effects between the dopants.[3,12] However, in the high-temperature doping process that uses boric acid and ammonia as the B and N precursors, boron nitride (BN) is inevitably formed; as BN is catalytically inactive for ORR and is electrically insulating, the overall performance of the resulting catalyst is compromised. Besides, if one considers the relatively poor ORR activity of graphene doped solely with B,[11] further improvement in performance could be expected if additional "active" elements were selected. Based on our recent work on the effect of the nanostructures of metal-free g-C_3N_4/C catalysts on ORR performance, relatively large and regular pores are more favorable than randomly formed inaccessible narrow pores;[9–11,13] these features have been rarely considered in studies on graphene-based materials for ORR.

Herein, we report for the first time the design and one-step synthesis of N and S dual-doped graphene (N-S-G) without the formation of any side products. The main focus of this research is to develop a high-performance metal-free ORR electrocatalyst to replace Pt/C as well as to gain insight into the synergistic effects originating from multiple-element doping. By selecting highly active S and N atoms as dopants, we achieved dual-doped N-S-G catalysts with excellent ORR performance comparable to that of commercial Pt/C and significantly better than that of graphene catalysts doped solely with S atoms (S-G) or with N atoms (N-G). Also, both dopant elements in N-S-G are efficiently utilized for ORR catalysis and do not form inactive compositions. The outstanding performance of N-S-G is explained by its dual activation of C atoms, as evidenced by both experimental data and quantum chemistry calculations. Moreover, we also used commercially available colloidal silica nanoparticles to create large mesopores for the first time in the graphene catalyst which are favorable for ORR since they facilitate mass transfer.[12] Besides, compared to the fuel-sensitive and vulnerable Pt/C, the proposed N-S-G material is much more tolerant to fuel crossover and displays long-term durability in alkaline environment. This N-S-G material not only presents a very promising substitute for expensive Pt/C as a low-cost fuel-cell catalyst, but it also has potential in other applications such as lithium–air batteries, photocatalysis, and heterocatalysis.

Mesoporous N-S-G was prepared through a one-step doping process as illustrated in Scheme 1. Graphene oxide (GO) was first prepared by Hummer's method and dispersed

[*] J. Liang, Y. Jiao, Prof. S. Z. Qiao
School of Chemical Engineering
The University of Adelaide, SA 5005 (Australia)
E-mail: s.qiao@adelaide.edu.au
M. Jaroniec
Department of Chemistry and Biochemistry
Kent State University, Kent, 44242 OH (USA)

[**] This work was financially supported by the Australian Research Council (ARC) through the Discovery Project program (DP1095861, DP0987969).

Supporting information for this article is available on the WWW under http://dx.doi.org/10.1002/anie.201206720.

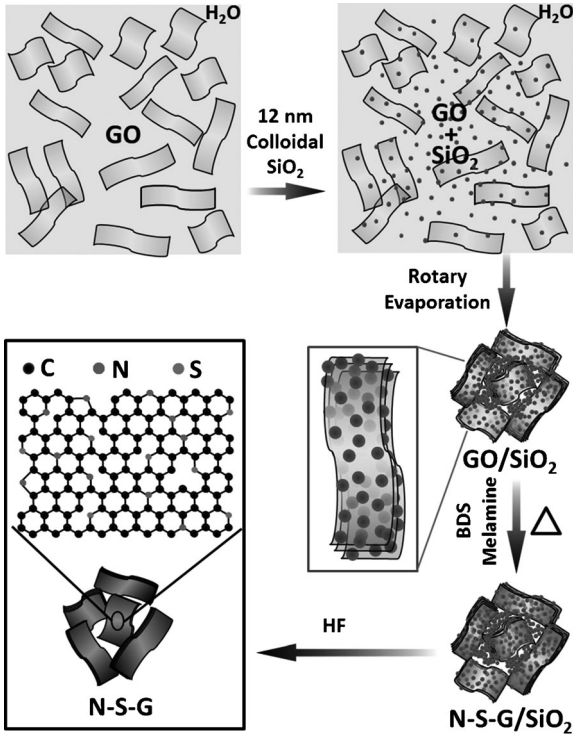

Scheme 1. Fabrication of N and S dual-doped mesoporous graphene (N-S-G) nanosheets from graphene oxide. See test for details.

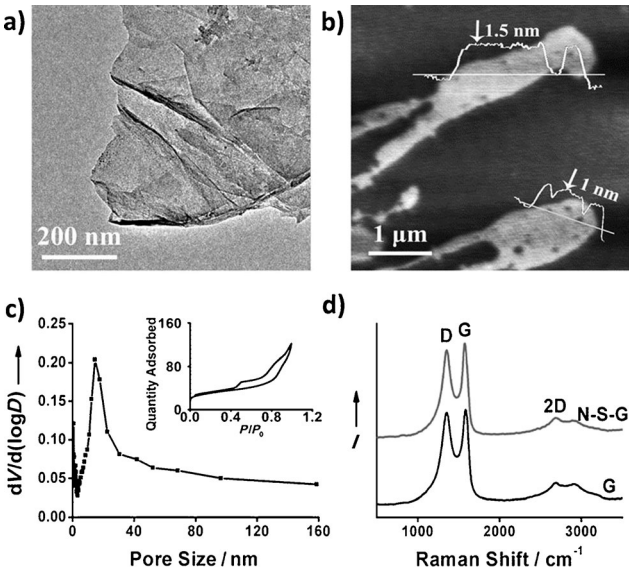

Figure 1. Characterization of typical N-S-G nanosheets. a,b) TEM and AFM images, respectively, c) pore size distribution and the corresponding nitrogen adsorption-desorption isotherms (inset), d) Raman spectra of N-S-G and pristine graphene (G).

in water.[14] Then commercial colloidal silica (12 nm), as the structural template, was added into the GO/water dispersion to achieve a SiO_2/GO weight ratio of 5:1. Water was removed by rotary evaporation, resulting in a brown crispy GO/SiO_2 composite. Melamine and benzyl disulfide (BDS) were selected as N and S precursors, respectively, and the doping process was carried out by heating the mixture of melamine/BDS/GO/SiO_2 (weight ratio of 5:5:1:5) at 900 °C in Ar to form N-S-G/SiO_2. The porous structure was formed in the N-S-G afterward by removing SiO_2 nanoparticles with hydrofluoric acid (HF). Mesoporous N-G and S-G, as well as pristine mesoporous graphene (G), were also prepared under similar conditions for comparison purposes.

The as-prepared mesoporous N-S-G was first investigated by transmission electron microscopy (TEM) and scanning electron microscopy (SEM) (images in Figure 1a and Figures S1 and S2 in the Supporting Information). Large amounts of transparent graphene nanosheets can be readily observed. Remarkably, the mesoporous N-S-G shows a very loose structure (Figures S1 and S2) similar to that of freeze-dried graphene aerogels but different from that of the typical densely packed graphene papers prepared without SiO_2.[15,16] Further structural details are also evident in the atomic force microscopy images (AFM) shown in Figure 1b and Figure S3. The AFM linear scan confirms that the thickness of a single graphene sheet is 1–1.5 nm, indicating 3–6 carbon atomic layers. Randomly located surface dents are also evident in the AFM image, which could result from defects in the doped graphene and might provide more high-energy edges that can act as active sites for ORR.

The porosity of N-S-G was investigated by nitrogen-adsorption technique. The nitrogen-adsorption isotherm of N-S-G (inset in Figure 1c) is of type IV with a distinct hysteresis loop in the medium- and high-pressure regions ($P/P_0 = 0.4$–1). The size of mesopores in the material range from 10 to 40 nm (Figure 1c, pore-size distribution calculated by the Barrett–Joyner–Halenda method); these are much larger than the mesopores in the previously reported graphene materials as a result of the silica template. These mesopores are expected to facilitate the diffusion of reactants in the ORR process.[13,17,18]

Further structural information about the doped graphene was obtained from Raman spectra (Figure 1d). A typical D band resulting from the disordered carbon atoms and a G band from sp^2-hybridized graphitic carbon atoms can be observed at roughly 1350 cm^{-1} and 1580 cm^{-1}, respectively.[12] Interestingly, the I_D/I_G ratio of N-S-G is similar to that of pristine graphene (G), which is lower than that of both N-G and S-G (Figure S4a), indicating larger crystalline graphitic domains in N-S-G.[19] The origin of these larger graphitic domains in the dual-doped graphene needs further study.

The doping of heteroelements into graphene was first probed by energy-dispersive spectrometry (EDS). The EDS spectrum indicates the presence of N, S, and O elements in graphene (Figure S4b), while the EDS elemental mapping of N and S, which is integrated onto the TEM image of the same region, illustrates a homogeneous distribution of S and N species in N-S-G (Figure 2a). Considering that both the N and S precursors were completely removed at temperatures below 750 °C in Ar, as shown by thermal gravimetric analysis (TGA) (Figure S5), it is reasonable to believe the N and S atoms belong to the doped graphene, rather than to any residual precursors. The chemical status of these elements was further investigated by X-ray photoelectron spectroscopy (XPS). The

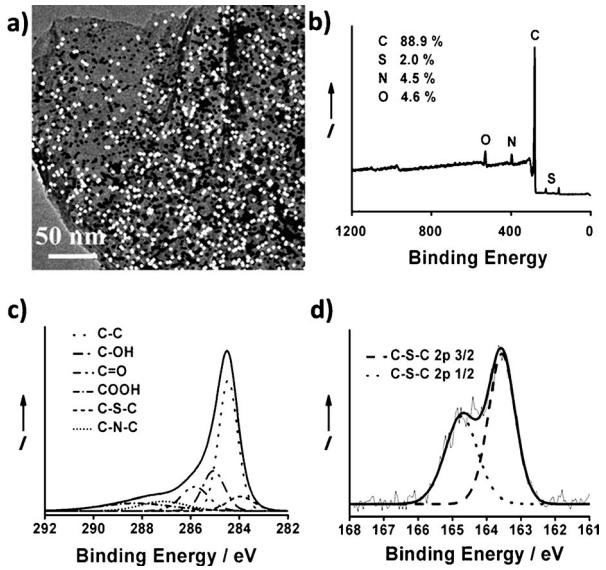

Figure 2. Compositional analysis of N-S-G. a) EDS elemental mapping indicating the distribution of N (black dots) and S atoms (white dots), b) XPS sweep scan, and the corresponding high-resolution spectra of c) C1s and d) S2p. The two peaks in (d) originate from the 2p 3/2 and 2p 1/2 splitting of the S2p spin orbital.

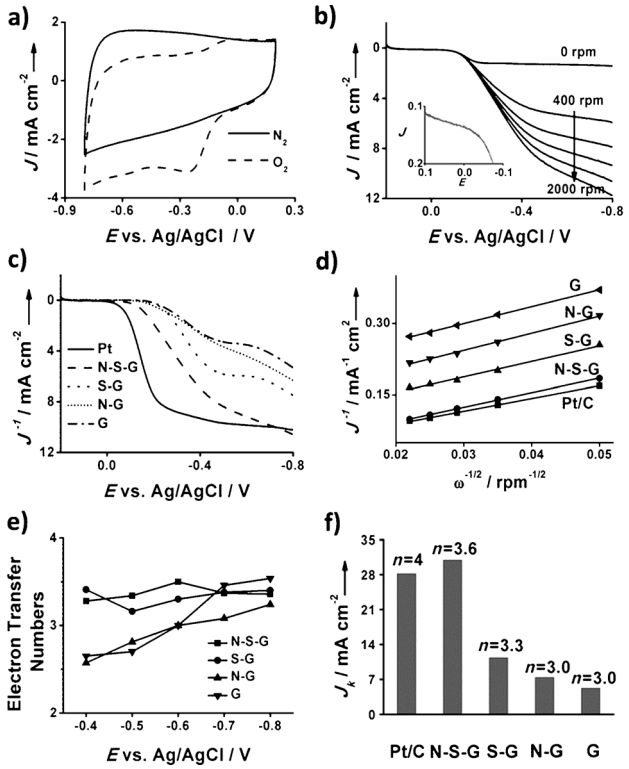

Figure 3. Electrochemical ORR catalytic performance of samples. a) CV curves of N-S-G in O_2- or N_2-saturated electrolyte. b) LSVs of N-S-G at different rotating speeds; the inset shows an enlargement of the initial region. c) LSVs of different samples at 1600 rpm. d) K-L plots of different samples at −0.6 V. e) Electron-transfer numbers as a function of the overpotential of different samples. f) Kinetic limiting current of different samples as well as the corresponding electron-transfer numbers at −0.6 V.

survey scan of N-S-G (Figure 2b) shows the identical elemental composition as that obtained from EDS. The N and S elemental content (4.5 atom % and 2.0 atom %, respectively) of the dual-doped N-S-G is comparable to that of the single-element-doped graphene materials (5.1 atom % of N in N-G and 1.3 atom % of S in S-G as shown in Figures S6a and S7a). The high-resolution spectrum of C1s in N-S-G (Figure 2c) can be deconvoluted into several single peaks, corresponding to C-S-C (283.9 eV)[20] and C-N-C (287.2 eV),[13,21] further confirming that N and S heteroatoms have been doped into the graphene framework. Different oxygen-containing groups (COOH, C=O, and C-OH) were also observed on N-S-G, similar to N-G, S-G, and pristine thermally reduced graphene (Figures S6b, S7b, and S9). Remarkably, N-S-G and S-G contain sulfur atoms that form thiophene-like structures with neighboring carbon atoms, as shown in the high-resolution S2p spectrum (Figure 2d and Figure S7c); SO_x groups, which are chemically inactive for ORR, are not evident.[9] On the other hand, the high-resolution N1s spectra of N-S-G and N-G (Figures S8 and S6c) show three nitrogen species, which are typically observed in the case of N-doped carbons.

The ORR catalytic performance of N-S-G was first investigated by cyclic voltammetry (CV) (Figure 3a); comparative studies were performed for N-G, S-G, and G (Figure S10). A quasi-rectangular voltammogram without obvious redox peak was obtained when the electrolyte was saturated with N_2, as a result of the the typical supercapacitance effect on porous carbon materials.[22,23] In contrast, when O_2 was introduced, a well-defined characteristic ORR peak, centered at −0.24 V with a reaction current of $-3.3\ mA\,cm^{-2}$, was observed with N-S-G. The ORR reaction current on N-S-G is apparently higher than on the solely doped N-G or S-G (Figure S10) or the pristine G. Moreover, the peak potential for N-S-G is also more positive than that of other recently reported metal-free ORR catalysts such as N-graphene,[17] S-graphene,[9] g-C_3N_4/C,[21] and co-doped graphenes,[12] indicating a more facile ORR process on this dual-heteroatom-doped N-S-G.

To gain additional insight about the ORR process on this dual-doped graphene, linear sweep voltammograms (LSVs) on a rotating disc electrode (RDE) were recorded at different rotating speeds from 0 rpm to 2000 rpm in 0.1M KOH electrolyte saturated with O_2; for the purpose of comparison, analogous LSV curves were obtained for N-G, S-G, and G as well as for commercial 20 wt % Vulcan Pt/C (Figure 3b and Figure S11). Typically, the current simultaneously increased as the potential became more negative, which is commonly observed on metal-free ORR catalysts with mesopores.[21] Remarkably, N-S-G displayed a very high ORR onset potential of −0.06 V (inset in Figure 3b), which is close to that of commercial Pt/C (−0.03 V) and much more positive than that of N-G, S-G, or G (ca. −0.18 V) (Figure 3c) at 1600 rpm. On the other hand, the ORR reaction current of N-S-G is also explicitly higher than that of other samples over the whole potential range, agreeing with the CV results. The more positive onset potential as well as the higher reaction current on N-S-G indicate that this material would have

clearly better catalytic performance and also supports the proposed synergistic effect caused by dual N and S doping.

To qualify the ORR process on this novel catalyst, the Koutecky–Levich (K-L) plots (J^{-1} vs, $\omega^{-1/2}$) were obtained for each sample from the reaction currents at −0.6 V on the LSVs at various rotating speeds (Figure 3d); the K-L plots were also obtained at other potentials as illustrated in Figure S12. The plots of all samples show good linearity, and noticeably, the N-S-G sample shows a high ORR current, which is very close to that of the commercial Pt/C catalyst and significantly higher than those of S-G, N-G, and pristine G at all rotation speeds; this is further indication of the outstanding ORR catalytic performance on the dually doped graphene as compared with the solely doped or nondoped materials. The electron-transfer numbers (n) of all the samples at different potentials were calculated according to the slopes of the linear fitted K-L plots on the basis of the K-L equation (Figure 3e; for details see the Supporting Information). Generally increasing n values were obtained for N-G, S-G, and G as the potential became more negative, while n for N-S-G was more stable and higher at 3.3–3.6 over most of the potential range. The higher and steadier electron-transfer numbers indicate a smoother and more electrochemically stable ORR process over N-S-G.

To more clearly determine the potential suitability of N-S-G as an ORR catalyst, we acquired the kinetic limiting current (J_k) from the intercept of the linearly fitted K-L plots at −0.6 V (Figure 3f) and at other potentials (Figure S12). Significantly, the J_k value of N-S-G exceeded that of commercial Pt/C at −0.6 V and was much superior to that of N-G, S-G, and G over the whole potential range. Taking into account that the J_k value of N-S-G is substantially higher than the summed value of N-G and S-G (corrected for heteroelement content), we believe that the excellent ORR performance is not simply the result of the superposition of the reaction currents due to N and S doping. Moreover, the J_k value of N-S-G sharply increased from 15 mA cm^{-2} to 52 mA cm^{-2} as the potential varied from −0.4 V to −0.8 V (Figure S12) and its value became nearly twice as high as that of Pt/C (52 mA cm^{-2} vs. 28 mA cm^{-2} at −0.8 V), which is a good indication that the potential current can be improved even further through structural modification.[13]

High selectivity towards ORR is important for potential fuel-cell catalysts to prevent possible fuel-crossover effects. In this study, the tolerance of N-S-G to methanol crossover was assessed in comparison with that of the commercial Pt/C catalyst (Figure S13a). When methanol was introduced into the testing cell, the current response of N-S-G remained unchanged, showing its high catalytic selectivity for ORR against methanol oxidation. In contrast, Pt/C showed an instantaneous current jump upon addition of methanol, reflecting its sensitivity to fuel crossover. The durability of N-S-G and Pt/C was also evaluated (Figure S13b). A 60 h test of N-S-G showed only a very slight performance attenuation of 19%. In contrast, the Pt/C catalyst suffered an activity loss of nearly 40%. The higher stability of the metal-free catalyst can be attributed to the strongly bonded heteroatoms in N-S-G and the improved chemical and mechanical stability of the mesoporous graphene relative to that of the carbon-black-based Pt/C, which could effectively prevent the loss of active sites.

The synergistic effect of the two dopants in enhancing ORR performance could be better studied and understood by employing density functional theory (DFT) calculations. Graphene networks doped by N and/or S atoms with different relative positions have been constructed for computational simulation as illustrated in Figure S14. Whether an atom can serve as an active site for ORR depends on both its charge density and spin density, with the latter playing a more important role than the former.[24] For N-G, which is doped solely by more electronegative N atoms (electronegativity of 3.04),[25] the ORR activity mainly originates from the surrounding C atoms with high charge density (0.27 in Figure S15a).[24,26] For S-G, the electronegativity of the S (2.58) and C atoms (2.55) are quite close, and the charge transfer between S and C is negligible.[27] Thus, the catalytic behavior is mainly affected by the mismatch of the outermost orbitals of sulfur and carbon (Figure S15b); then the S atom is positively charged and hence can be viewed as the catalytic center for ORR.[9] Remarkably, when S and N are simultaneously incorporated into graphene to form dual-doped N-S-G, the maximum spin density is substantially uplifted to 0.43 (C1 in Figure 4) indicating significantly elevated ORR activity. A larger number of active C atoms is also observed (S and C1–C5 as shown in Figure 4),[24] because the dual-doping of S and N introduces asymmetrical spin and charge density. Simulations performed for other N-S-G models with different relative positions of the S and N atoms (Figure S16–19) also show that the charge/spin densities are increased to a certain extent, indicating higher ORR catalytic performance. All these features, including both higher activity and more active sites, can well explain the significant enhancement of ORR catalytic activity such as the more positive onset potential and higher reaction current on N-S-G relative to that on N-G or S-G.

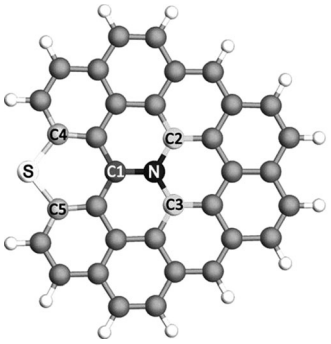

Atom Number	Spin Density	Charge Density
C1	0.43	0.23
C2	-0.03	0.28
C3	-0.03	0.28
C4	0.16	-0.22
C5	0.16	-0.22
N	0.06	-0.88
S	0.09	0.21

Figure 4. Spin and charge density of graphene network (gray) dual-doped by N (black) and S (white). C1 has very high spin density, C2 and C3 have high positive charge density, and C4 and C5 have moderately high positive spin densities.

In summary, we have described the first design and preparation of N and S dual-doped mesoporous graphene as a metal-free catalyst for ORR. This novel material shows

excellent catalytic activity including a highly positive onset potential and very high kinetic limiting current, which makes it closely comparable to the commercial Pt/C catalyst. The DFT calculations have revealed that the synergistic performance enhancement results from the redistribution of spin and charge densities brought about by the dual doping of S and N atoms, which leads to a large number of carbon atom active sites. This catalyst also shows a full fuel tolerance and much better long-term stability than Pt/C in alkaline environment. Moreover, this material can be prepared by a very simple one-step doping process using solid and low-cost precursors, and its porosity is introduced by employing commercially available colloidal silica; thus, it is easily adaptable for large-scale synthesis. Because of all these outstanding features, it is expected that the N-S-G material will be a very suitable catalyst for the next generation of fuel cells, and should find other applications as well such as in lithium–air batteries, photocatalysis, oxygen sensors, and water treatment.

Received: August 20, 2012
Published online: October 10, 2012

Keywords: graphene · heterogeneous catalysis · nanostructures · oxygen reduction reaction · synergistic effects

[1] B. C. H. Steele, A. Heinzel, *Nature* **2001**, *414*, 345.
[2] E. M. Erickson, M. S. Thorum, R. Vasic, N. S. Marinkovic, A. I. Frenkel, A. A. Gewirth, R. G. Nuzzo, *J. Am. Chem. Soc.* **2012**, *134*, 197.
[3] S. Wang, E. Iyyamperumal, A. Roy, Y. Xue, D. Yu, L. Dai, *Angew. Chem.* **2011**, *123*, 11960; *Angew. Chem. Int. Ed.* **2011**, *50*, 11756.
[4] R. Bashyam, P. Zelenay, *Nature* **2006**, *443*, 63.
[5] H. Gasteiger, N. Markovi, *Science* **2009**, *324*, 48.
[6] S. Maldonado, K. J. Stevenson, *J. Phys. Chem. B* **2005**, *109*, 4707.
[7] H. Wang, T. Maiyalagan, X. Wang, *ACS Catal.* **2012**, *2*, 781.
[8] A. Fasolino, J. H. Los, M. I. Katsnelson, *Nat. Mater.* **2007**, *6*, 858.
[9] Z. Yang, Z. Yao, G. Li, G. Fang, H. Nie, Z. Liu, X. Zhou, X. a. Chen, S. Huang, *ACS Nano* **2012**, *6*, 205.
[10] Z. Yao, H. Nie, Z. Yang, X. Zhou, Z. Liu, S. Huang, *Chem. Commun.* **2012**, *48*, 1027.
[11] L. Yang, S. Jiang, Y. Zhao, L. Zhu, S. Chen, X. Wang, Q. Wu, J. Ma, Y. Ma, Z. Hu, *Angew. Chem.* **2011**, *123*, 7270; *Angew. Chem. Int. Ed.* **2011**, *50*, 7132.
[12] S. Wang, L. Zhang, Z. Xia, A. Roy, D. W. Chang, J. B. Baek, L. Dai, *Angew. Chem.* **2012**, *124*, 4285; *Angew. Chem. Int. Ed.* **2012**, *51*, 4209.
[13] J. Liang, Y. Zheng, J. Chen, J. Liu, D. Hulicova-Jurcakova, M. Jaroniec, S. Z. Qiao, *Angew. Chem.* **2012**, *124*, 3958; *Angew. Chem. Int. Ed.* **2012**, *51*, 3892.
[14] W. S. Hummers, R. E. Offeman, *J. Am. Chem. Soc.* **1958**, *80*, 1339.
[15] S. Stankovich, D. A. Dikin, R. D. Piner, K. A. Kohlhaas, A. Kleinhammes, Y. Jia, Y. Wu, S. T. Nguyen, R. S. Ruoff, *Carbon* **2007**, *45*, 1558.
[16] F. Liu, S. Song, D. Xue, H. Zhang, *Adv. Mater.* **2012**, *24*, 1089.
[17] S. Yang, L. Zhi, K. Tang, X. Feng, J. Maier, K. Müllen, *Adv. Funct. Mater.* **2012**, DOI: 10.1002/adfm.201200186.
[18] S. Yang, X. L. Feng, X. C. Wang, K. Mullen, *Angew. Chem.* **2011**, *123*, 5451; *Angew. Chem. Int. Ed.* **2011**, *50*, 5339.
[19] M. Jin, T. H. Kim, S. C. Lim, D. L. Duong, H. J. Shin, Y. W. Jo, H. K. Jeong, J. Chang, S. Xie, Y. H. Lee, *Adv. Funct. Mater.* **2011**, *21*, 3496.
[20] S. Wan, L. Wang, Q. Xue, *Electrochem. Commun.* **2010**, *12*, 61.
[21] Y. Zheng, Y. Jiao, J. Chen, J. Liu, J. Liang, A. Du, W. Zhang, Z. Zhu, S. C. Smith, M. Jaroniec, G. Q. Lu, S. Z. Qiao, *J. Am. Chem. Soc.* **2011**, *133*, 20116.
[22] R. Liu, D. Wu, X. Feng, K. Müllen, *Angew. Chem.* **2010**, *122*, 2619; *Angew. Chem. Int. Ed.* **2010**, *49*, 2565.
[23] W. Yang, T.-P. Fellinger, M. Antonietti, *J. Am. Chem. Soc.* **2011**, *133*, 206.
[24] L. Zhang, Z. Xia, *J. Phys. Chem. C* **2011**, *115*, 11170.
[25] A. L. Allred, *J. Inorg. Nucl. Chem.* **1961**, *17*, 215.
[26] K. Gong, F. Du, Z. Xia, M. Durstock, L. Dai, *Science* **2009**, *323*, 760.
[27] S. Glenis, A. J. Nelson, M. M. Labes, *J. Appl. Phys.* **1999**, *86*, 4464.

